On the Application of Coupled Mode Theory for Modeling Fiber Bragg Gratings

Martin McCall , *Member, OSA*

***Abstract*—We remove some ambiguities associated with the coupled mode description of light propagation in fiber Bragg gratings (FBG's). We show, in particular, that different methods employed in the literature lead to physically distinct results. The significant distinctions are discussed both for interferometric systems and intensity-only spectral measurements. Analysis of the reflection spectrum of a suitably designed double-grating structure is shown to result in a novel form of spectral hole, similar to the well-known effect derived from discontinuous phase gratings.**

***Index Terms*—Bragg gratings, coupled mode theory.**

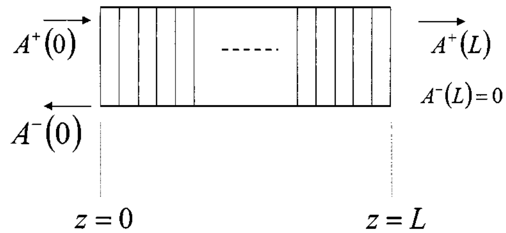

Fig. 1. Interaction geometry for FBG's.

I. Introduction

FIBER Bragg gratings (FBG's), or gratings recorded along the core of photosensitive fiber, are currently showing considerable potential as passive integrated devices in photonics. Gratings within fibers offer the possibility of chromatic and environmentally sensitive reflectivity which is of significance both to the sensor and optical communications communities. A single uniform grating has limited application, however, as just a single Bragg stop band is defined, and, moreover, the side-bands are rather high resulting in a low rejection ratio. Hence, considerable effort has now been directed at modifying the simple grating structure to improve or specialize its characteristics. This research has moved in several directions. Coupling into cladding modes in long-wavelength gratings has, for example, introduced additional degrees of freedom so that temperature/strain deformations can be distinguished. Several cascaded gratings of different wavelength introduce several stop bands for wavelength division multiplexing, while chirped gratings give spatially dispersed reflectivity for temporal shaping and improved spectral characteristics [1], [2]. Another idea has been the introduction of abrupt phase discontinuities within the grating, to produce sharp intraband spectral features [3], [4]. This has been most successfully employed in so-called quarter wavelength shifted distributed feedback lasers, where the narrow resonance provides single mode operation. As applications of this concept now move on to the consideration of multiple discontinuities [6], it is especially important to obtain a sound theoretical description. Despite its well-documented limitations, coupled mode theory (CMT) remains the most widely used tool for analyzing simple grating structures. Discontinuities of grating phase, pitch and amplitude fit in well with this prescription, as they effectively define a series of uniform gratings which can separately be treated using CMT. It is our intention in this paper to analyze critically how different literature formulations of CMT applied to Bragg gratings are *not* equivalent and can lead to physically distinct results, due to the omission, in some cases, of dephasing terms. For pitch discontinuities it is shown that under suitable conditions an apparently novel form of intraband gap spectral hole results. For phase discontinuities a similar anomaly arises where inequivalent complex coupling constant and phase matrix methods are employed. Although in this case all reflectivity/transmission calculations yield identical results using the different methods, interferometric systems sensitive to the phase difference between the incident and scattered waves yield distinct phenomena.

In Section II, we formulate the standard CMT description and give the general solution with arbitrary starting point on the initial values. Through a dephasing transformation it is shown how the various previous formulations relate to one another, and how they are applied to multiple gratings. We also compare the complex-coupling-constant and phase matrix descriptions of grating phase discontinuities. In Section III, we calculate various response functions of systems in which the physical significance between the various methods is exposed. Finally, in Section IV, we conclude with a few applications suggestions.

II. Formulation

Referring to Fig. 1, the standard coupled wave formulation for forward/backward wave amplitudes, $A^{\pm}$, of propagation constant β propagating in a single-mode fiber within which is written a Bragg grating of wavenumber $K = 2\pi/\Lambda$, is given by

$$\frac{d}{dz}\begin{bmatrix} A^+ \\ A^- \end{bmatrix} = i\begin{bmatrix} 0 & \kappa e^{-i\delta\beta z} \\ -\kappa^* e^{i\delta\beta z} & 0 \end{bmatrix}\begin{bmatrix} A^+ \\ A^- \end{bmatrix} \tag{1}$$

where $\delta\beta = 2\beta - K$ is the detuning from Bragg resonance, $|\kappa| = (\pi^2\delta\epsilon/\beta\lambda_0^2) = (\pi\delta n/\lambda_0 n_{\text{eff}})$, is the grating coupling constant, $\delta\epsilon$ being the amplitude of the dielectric modulation, δn the index modulation, n_{eff} the effective mode index and λ_0 the free-space wavelength. The phase ofκ codes the grating phase.

Manuscript received July 7, 1999; revised October 26, 1999. This work was supported by EPSRC under Grant GM/4746.

The author is with the Imperial College, London SW7 2BZ, U.K.

Publisher Item Identifier S 0733-8724(00)01319-0.

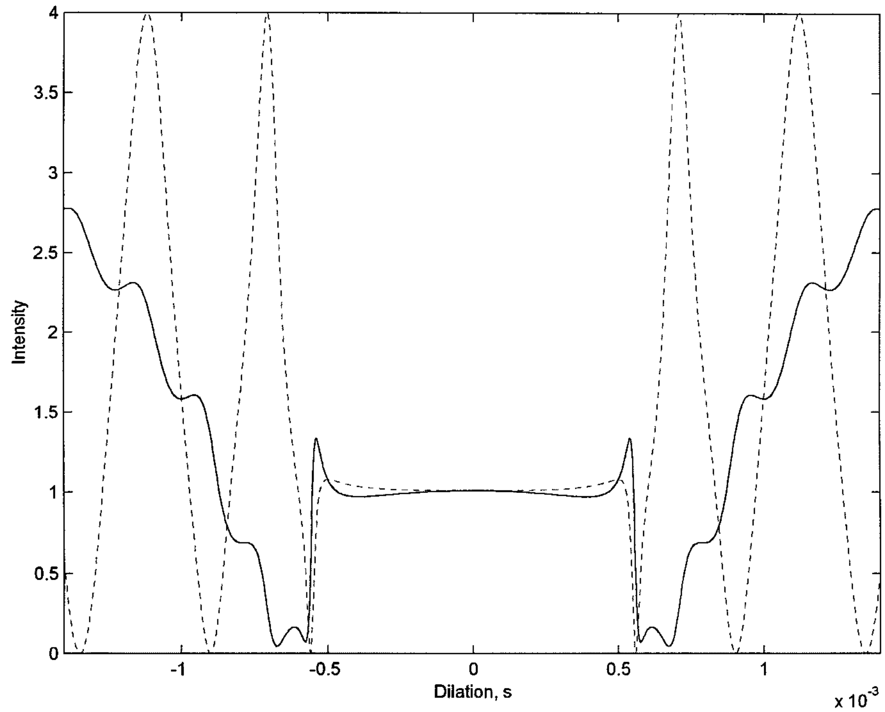

Fig. 2. Mach–Zehnder response function versus grating dilation factor $s = \delta L/L$. (a) Solid line: Including dephasing inversion matrix $M^{-1}(L)$. (b) Broken line: Omitting the dephasing inversion matrix $M^{-1}(L)$. Parameters: $\lambda = 1.5\mu$m, $\delta n_{\rm eff} = 10^{-3}$, $n_{\rm eff}L = 3$ mm.

Defining the column vector $A(z) = [A^+(z), A^-(z)]^T$, the general solution to (1) may be expressed as

$$A(z) = S(l_0, z)A(l_0) \tag{2}$$

where

$$S(l_0, z) \equiv \begin{bmatrix} e^{-i\delta\beta(z-l_0)/2}p & e^{-i\delta\beta(z+l_0)/2}q \\ e^{i\delta\beta(z+l_0)/2}q^* & e^{i\delta\beta(z-l_0)/2}p^* \end{bmatrix} \tag{3}$$

$p(z - l_0)$ and $q(z - l_0)$ being given by

$$p(z - l_0) = \left[\cosh[\Delta(z - l_0)] + i\,\frac{\delta\beta}{2\Delta}\,\sinh[\Delta(z - l_0)]\right] \tag{4}$$

$$q(z - l_0) = i\,\frac{\kappa}{\Delta}\,\sinh[\Delta(z - l_0)] \tag{5}$$

and $\Delta \equiv [|\kappa|^2 - (\delta\beta/2)^2]^{1/2}$. We have here, unlike some authors ([5], [7], [8], [10], though not [9]), emphasized the dependence of the scattering matrix S on the point l_0 at which the amplitudes $A(l_0)$ are presumed known. We prefer the form given in (2)–(5), as in this form it is clear that moving the initial point from $z = 0$ to l_0 is *not* described by replacing z with $z - l_0$ in the solution when $A(0)$ is given. Usually, $l_0 = 0$, however, in which case the above reduces to the well-known form given in the previous literature (in, e.g., [5]). In the above notation the resultant scattering matrix of N gratings in series is given by

$$S(0, L) = S_N(z_{N-1}, z_N) \cdots S_2(z_1, z_2) \cdot S_1(z_0, z_1) \tag{6}$$

where $z_0 = 0$ and $z_N = L$. The above solution also emphasizes the following necessary property for an arbitrary point $z = l$ (where $0 < l < L$), for a single grating of length

$$S(0, L) = S(l, L) \cdot S(0, l) \tag{7}$$

as may be verified by direct calculation from (2) to (5). By applying the condition $A^-(L) = 0$

$$A^-(0) = -\frac{q^*(L)}{p^*(L)}\,A^+(0) \tag{8}$$

after which the grating reflectivity and transmission are easily calculated.

Some authors ([8], [10]–[12]) have solved this problem using the transformation $\tilde{A} = M \cdot A$, where

$$M = \begin{bmatrix} e^{i\delta\beta z/2} & 0 \\ 0 & e^{-i\delta\beta z/2} \end{bmatrix}. \tag{9}$$

In this frame, equation (1) takes the autonomous form

$$\frac{d\tilde{A}}{dz} = i\begin{bmatrix} \delta\beta/2 & \kappa \\ -\kappa^* & -\delta\beta/2 \end{bmatrix} \cdot \tilde{A}. \tag{10}$$

The solution is

$$\tilde{A}(z - l) = \tilde{S}(z - l)\tilde{A}(l) \tag{11}$$

where

$$\tilde{S}(z) = \begin{bmatrix} p(z) & q(z) \\ q^*(z) & p^*(z) \end{bmatrix} \tag{12}$$

where $p(z)$ and $q(z)$ were defined previously.

The two scattering matrices S and $\tilde{S}$ are related by

$$S(L, z) = M^{-1}(z) \cdot \tilde{S}(z - l) \cdot M(l). \tag{13}$$

Thus when considering multiple gratings, it is clear that sandwiched between $\tilde{S}_{i+1}(z_{i+1} - z_i)$ and $\tilde{S}_i(z_i - z_{i-1})$ is the matrix

$$N_{i,j+1}(z_i) = M_{i+1}(z_i) \cdot M_i^{-1}(z_i). \tag{14}$$

This matrix, which is evidently only relevant to gratings of dissimilar pitch (so that $\delta\beta_{i+1} \neq \delta\beta_i$), is often apparently ignored in calculations ([8], [10], [11]) and it is presumed that multiple gratings are described by the product $\tilde{S}_N \cdot \tilde{S}_2 \cdot \tilde{S}_1$. How-

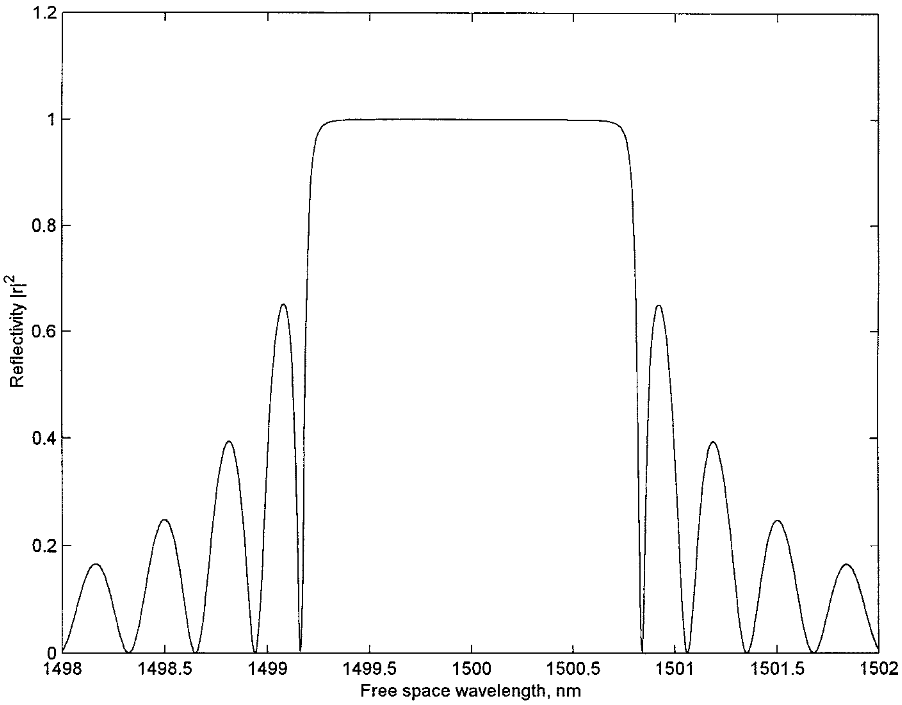

Fig. 3. Grating reflectivity spectrum. Solid line: Including the inversion dephasing matrix $M^{-1}(L)$. Broken line: Omitting the inversion dephasing matrix $M^{-1}(L)$. Parameters as for Fig. 2.

ever, as shown in Section III, this procedure leads to scattered amplitudes which differ from those calculated when the $N_{i,j+1}$, together with the final inversion $M_N^{-1}(L)$, is included.

A similar, but distinct anomaly occurs when considering two identical gratings delineated by a phase discontinuity. The presence of phase discontinuities within a Bragg grating effectively divides the structure into several subgratings. As noted above (1) grating discontinuities may be accounted for by complexifying the grating coupling constant ([5], [8], [9]). If the phase change at a discontinuity at $z = L$ is 2ϕ (the factor of two is for convenience), then the resultant scattering over the length L of the grating is described by

$$S(l, L, \phi) \cdot S(0, l, 0) \tag{15}$$

where for the second grating, $\kappa \rightarrow \kappa e^{-2i\phi}$ so that

$$q(z-l) \rightarrow q(z-l, \phi) = i\,\frac{\kappa}{\Delta}\,e^{-i2\phi}\,\sinh[\Delta(z-l)]. \tag{16}$$

$p(z-l)$ is unaffected.

An alternative approach used ([7], [10], [11]) is to keep κ real and account for phase discontinuities via phase matrices of the form

$$\Phi_j = \begin{bmatrix} e^{i\phi_j} & 0 \\ 0 & e^{-i\phi_j} \end{bmatrix} \tag{17}$$

the resultant scattering matrix for several discontinuities then being given by

$$\left[\prod_{j=1}^{N} S(z_j, z_{j+1}) \cdot \Phi_j\right] \cdot S(0, z_1). \tag{18}$$

However, as discussed below, this also leads to scattered amplitudes which differ in phase with respect to those calculated by complexifying κ.

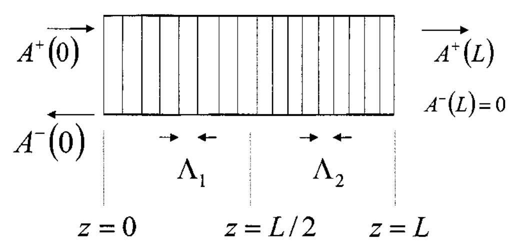

Fig. 4. Two gratings of dissimilar pitch.

III. Results

The simplest context within which these issues are exposed is that of a single grating (Fig. 1), for $M^{-1}(L)$ which the scattering matrices of (3) and (12) differ by the detuning inversion matrix. We contrast the two methods by calculating the output of an equal path Mach–Zehnder interferometer, in which the incident and transmitted waves are interfered

$$\begin{aligned} &|A^+(0) + A^+(L)|^2 \\ &\quad = |e^{-i\delta\beta L/2}\tilde{A}^+(0) + e^{i\delta\beta L/2}\tilde{A}^+(L)|^2 \end{aligned}$$

and compare this with $|\tilde{A}^+(0) + \tilde{A}^+(L)|^2$. The detuning can equivalently be induced by either changing the wavelength, or by dilating the grating. A fractional change in the grating length of $s = \delta L/L$ creates a similar deformation of the grating period $s = \delta\Lambda/\Lambda$. This can be induced either by strain or temperature increase and produces the same detuning as a change in wavelength of $\delta\lambda = \lambda^2[\lambda + 2L\Lambda(1-1/s)]^{-1}$. As well as sensing, we also note the relevance of these considerations to Mach–Zehnder-based interferometric add–drop filters ([15]). Fig. 2 shows the intensity as a function of the strain using the two methods. Outside the stopband, with the detuning omitted [see Fig. 2(b)], the response is nearly periodic, while with the detuning matrix

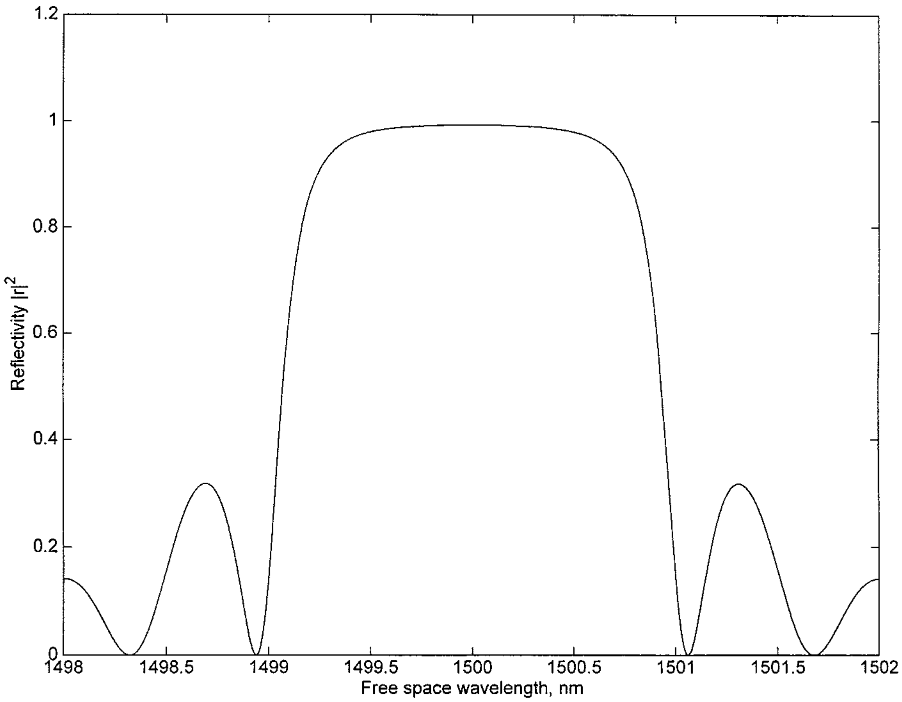

Fig. 5. Reflection spectra for two gratings of dissimilar pitch. $\Lambda_2 = 0.75\Lambda_1$, other parameters as for Fig. 2: (a) with intermediate dephasing matrix $N_{1,2}(L/2)$ and (b) without intermediate dephasing matrix $N_{1,2}(L/2)$.

at large detuning, the output is a constant value given by constructive interference. This is also clear from looking at the large detuning limit ($|\delta\beta| \gg |\kappa|$) when the scattering matrix S becomes the identity.

We note that, in this case, both methods yield the same grating transmission and reflection spectra which for completeness we give in Fig. 3. This shows the spectrum at zero dilation, though as noted above dilation and wavelength changes are equivalent.

We now turn to the case of two gratings of dissimilar pitch (see Fig. 4). Choosing parameters as for the above calculations, but with the second grating with a different period ($\Lambda_2 = 0.75\Lambda_1$), we obtain, for the two calculation methods, the reflection spectra illustrated in Fig. 5, the spectrum showing the expected reduction in finesse. The spectra are almost identical, and appear to be so for large parameter ranges. However, as noted above, the two methods differ by the intermediate matrix

$$N_{1,2}(L/2) = \begin{bmatrix} e^{-i(\delta\beta_2 - \delta\beta_1)L/4} & 0 \\ 0 & e^{+i(\delta\beta_2 - \delta\beta_1)L/4} \end{bmatrix}. \quad (19)$$

This is similar to the phase discontinuity matrix equation (17), which is known to yield spectral holes whenever $\phi_j = \pi/2$. Thus, in this case, we expect a spectral hole to appear whenever

$$\frac{1}{\Lambda_1} - \frac{1}{\Lambda_2} = \frac{1}{L}. \quad (20)$$

Detailed algebraic considerations show this to be the case. With similar parameters as before, but with $\Lambda_1 = 0.51774$ μm and $\Lambda_2 = 0.51761$ μm (which is the condition (20) for a grating with $n_{\text{eff}}L = 3$ mm, with n_{eff} taking the typical value of 1.4486), without dephasing terms [see Fig. 6(b)] no spectral hole is seen, while with the intermediate dephasing matrix [Fig. 6(a)], a spectral hole occurs at the average Bragg wavelength $\lambda = n_{\text{eff}}(\Lambda_1 + \Lambda_2) = 1.4998$ μm. Otherwise, the spectra for the two calculation methods are very similar. This method of producing intraband spectral holes is apparently novel, and may have significant fabricational advantages over the traditional method using phase discontinuities. Moreover, the concept is applicable to other periodic media (e.g., chiral thin films) and is currently undergoing further theoretical and experimental investigation [13], [14].

We finally consider a single grating phase discontinuity located at $z = l$—see Fig. 7.

For the complex-coupling-constant method, setting $(p_{1,2}, q_{1,2})$ to be the respective matrix elements of $S(0, l, 0)$ and $S(l, L, \phi)$, we have for the matrix elements of the resultant matrix S

$$(p, q) = (p_1 p_2 + q_1^* q_2, q_1 p_2 + p_1^* q_2). \quad (21)$$

For the phase matrix method, p_1, p_2 and q_1 are as above, but q_2 no longer contains the grating phase and is denoted $\tilde{q}_2$. The matrix elements of the resultant matrix, $\tilde{S}$, in this case are

$$(\tilde{p}, \tilde{q}) = (p_1 p_2 e^{i\phi} + q_1^+ \tilde{q}_2 e^{-i\phi}, q_1 p_2 e^{i\phi} + p_1^* \tilde{q}_2 e^{-i\phi}). \quad (22)$$

The inequivalence of the two formulations is shown from the fact that

$$\tilde{S} = \Phi \cdot S \quad (23)$$

provided $q_2 = \tilde{q}_2 e^{-2i\phi}$. The two formulations thus yield output amplitudes $\tilde{A}(L) = \Phi \cdot A(L)$. Evidently calculations of the reflectivity $(= |A^-(0)/A^+(0)|^2)$ and transmission $(= |A^+(L)/A^+(0)|^2)$ will be unaffected, but any setup in which the transmitted/reflected amplitudes are interfered with the incident wave, will yield distinct results. As for the case of a single grating, we illustrate by calculating the transmission

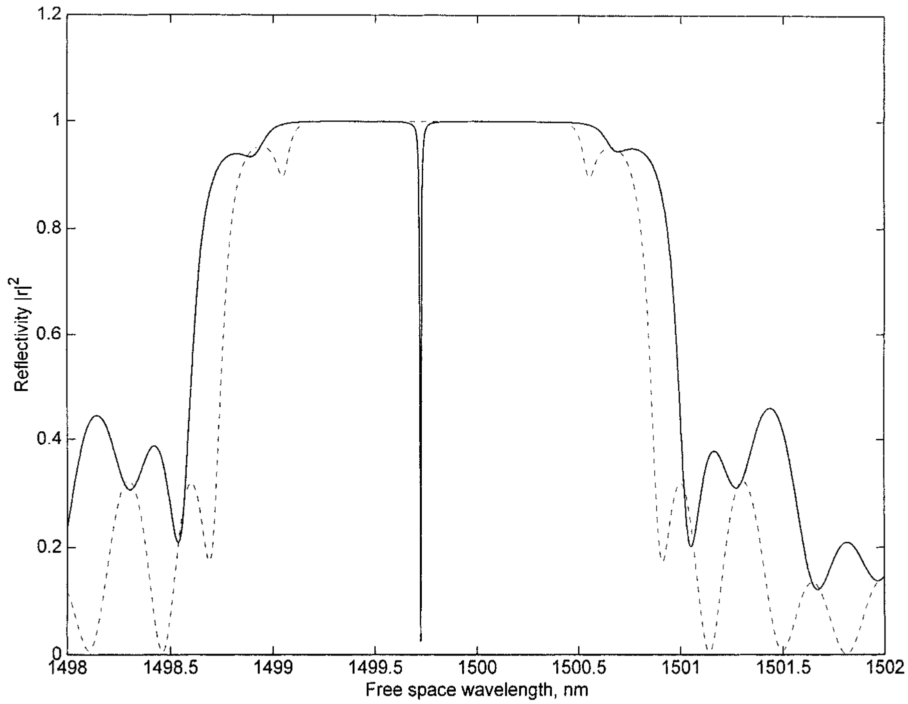

Fig. 6. Reflection spectra for two gratings of slightly dissimilar pitch for which the condition $1/\Lambda_1 - 1/\Lambda_2 = 1/L$ is fulfilled (see text). $\Lambda_1 = 0.5177$ μm and $\Lambda_2 = 0.5179$ μm other parameters as for Fig. 2: (a) Solid line: with intermediate dephasing matrix $N_{1,2}(L/2)$, (b) Broken line: without intermediate dephasing matrix . Note that the spectral hole is slightly detuned from the Bragg resonance for grating 1.

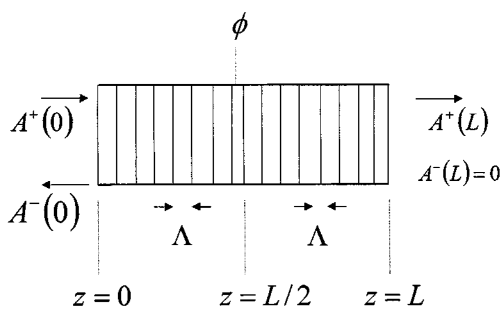

Fig. 7. Single grating phase discontinuity.

resulting from combining $A^+(L)$ with $A^+(0)$ in an equal path Mach–Zehnder interferometer (MZI)

$$I(\phi) = |A^+(0) + A^-(L)|^2. \tag{24}$$

In practice the phase discontinuity may be produced by a uniform "gap" between the two gratings, the length of the gap determining the phase difference between the two gratings. It is thus relevant to explore the intensity $I(\phi)$ as a function of the phase of the discontinuity, as the latter may be induced via environmental effects (e.g., temperature, or strain) which change the length of the gap.

The results for the two methods for a phase discontinuity placed at the midpoint are shown in Figs. 8 and 9. In this case we plot the response as a function of the phase of the discontinuity. Fig. 8 shows the reflection characteristic illustrating the well-known appearance of a spectral hole $\phi = \pi/2$. The curve is the same for both methods. The Mach–Zehnder response (Fig. 9), however, shows quite distinct characteristics for the complex-coupling-constant method, and the phase matrix method. Similar results are obtained when interfering the reflected beam with the incident beam, or interfering the reflected beam with the transmitted beam.

IV. Conclusion

We have formulated precisely the general solution to the Bragg grating problem, giving due regard to form of the solution under spatial translations and noting variations within the literature. We have demonstrated that modeling phase discontinuities in fiber-Bragg gratings using phase matrices Φ, can lead to erroneous results in any experiment sensitive to the phase of the transmitted or reflected beams. The correct method is to code phase differences between gratings as a phase constant in the grating coupling constant, κ. Some authors have used combinations of methods (e.g., in [8] the authors work solely in the $\tilde{A}$ frame, but use complexκ for phase discontinuity). We have demonstrated that these distinctions, though apparently trivial, result in distinct results when analysing the transmission of a MZI. Such results are of potential significance in sensor applications ([15]). An issue in the use of Mach–Zehnder fiber sensors is to relate the measured transmission to *the location* of an environmental change within one arm of the interferometer. The inclusion of a grating in one arm, within which phase continuities exist may be able to address this problem, for which the correct calculation of the transmission function is highly significant.

The apparently novel method of producing intraband spectral holes discussed in this paper may have significant advantages over phase discontinuity methods. Many Bragg gratings are produced holographically and it is relatively simple to change recording parameters such as interaction angle or wavelength, whereas phase discontinuity methods require considerable

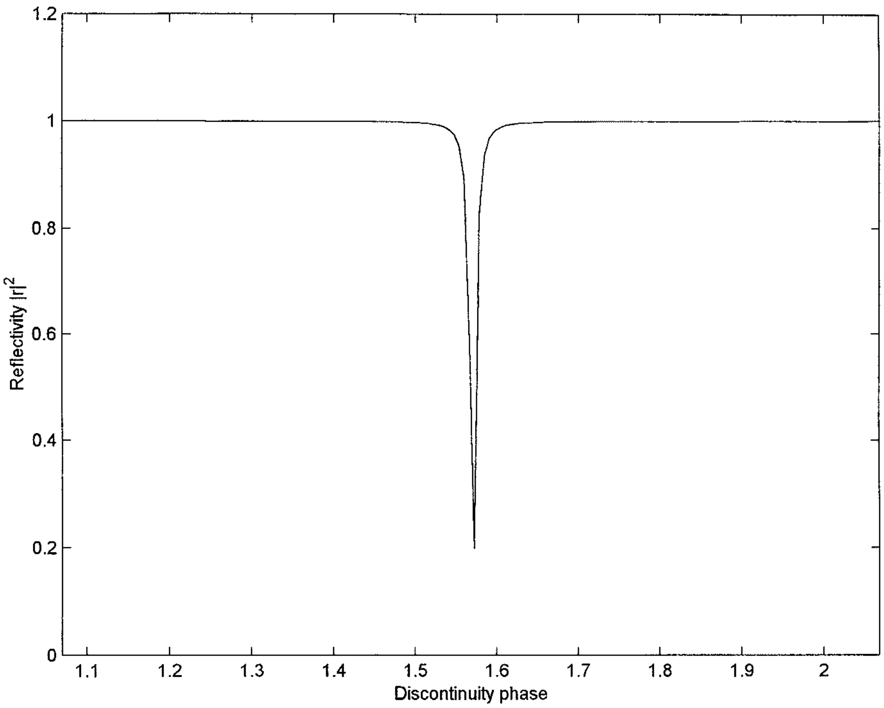

Fig. 8. Reflectivity versus phase of discontinuity for a phase discontinuity at the mid-point of grating. Incident wavelength is for Bragg resonance $\lambda = 1.5\mu$m. (a) Solid line: Complex grating coupling constant method. (b) Broken line: Phase matrix method. Parameters as for Fig. 2.

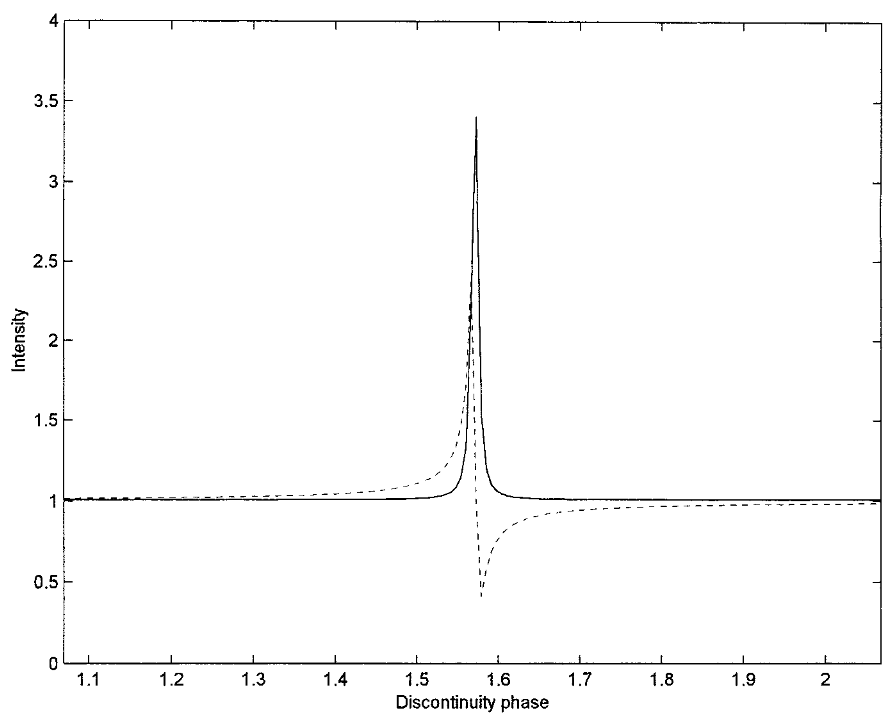

Fig. 9. Equal-path Mach–Zehnder response versus phase of discontinuity placed at mid-piont of grating. Incident wavelength is for Bragg resonance $\lambda = 1.5\mu$m. (a) Solid line: Complex grating coupling constant method. (b) Broken line: Phase matrix method. Parameters as for Fig. 2.

positional accuracy. Furthermore, ultraviolet (UV) curing provides a very convenient postprocessing method of changing the pitch of part of a grating structure. We also note that (20) indicates that the spectral hole is induced for a *small* change in the grating pitch. This could thus form the basis of a novel sensitive sensor in which an initially uniform grating is locally dilated by strain/temperature variations.

We will explore these issues in a further publication.

ACKNOWLEDGMENT

The author would like to thank Dr K. Weir for a useful discussion.

REFERENCES

[1] G. E. Town, K. Sugden, J. A. R. Williams, I. Bennion, and S. B. Poole, "Wide-band Fabry-Perot-like filters in optical fiber," *IEEE Photon. Technol. Lett.*, vol. 7, no. 4, pp. 78–80, Jan. 1995.

[2] L. Zhang, K. Sugden, I. Bennion, and A. Molony, "Wide-stopband chirped fiber moiré grating transmission filters," *Elec. Lett.*, vol. 31, pp. 477–479, Mar. 1995.

[3] J. Canning and M. G. Sceats, "π-phase-shifted periodic distributed structures in optical fibers by UV post-processing," *Electron. Lett.*, vol. 30, pp. 1344–1345, Aug. 1994.

[4] R. Kashyap, P. F. Mckee, and D. Armes, "UV written reflection grating structures in photosensitive optical fibers using phase-shifted phase masks," *Electron. Lett.*, vol. 30, pp. 1977–1978, Nov. 1994.

[5] M. Yamada and K. Sakuda, "Analysis of almost-periodic distributed feedback slap waveguides via a fundamental matrix approach," *Appl. Opt.*, vol. 26, pp. 3474–3478, Aug. 1987.

[6] F. Bakhti and P. Sansonetti, "Wide bandwidth, low loss and highly rejective doubly phase-shifted UV-written fiber bandpasss filter," *Electron. Lett.*, vol. 32, pp. 581–582, 1986.

[7] L. Wei and W. Lit, "Phase-shifted Bragg grating filters with symmetrical structures," *J. Lightwave Technol.*, vol. 15, pp. 1405–1410, Aug. 1997.

[8] R. Zengerle and O. Leminger, "Phase-shifted Bragg-grating filters with improved transmission characteristics," *J. Lightwave Technol.*, vol. 13, pp. 2354–2358, Dec. 1995.

[9] F. Bakhti and P. Sansonetti, "Design and realization of multiple quarter-wave phase-shifts UV-written bandpass filters in optical fibers," *J. Lightwave Technol.*, vol. 15, pp. 1433–1437, Aug. 1997.

[10] G. P. Agrawal and S. Radic, "Phas-shifted fiber Bragg gratings and their applications for wavelength demultiplexing," *IEEE Photon. Technol. Lett.*, vol. 6, pp. 995–997, Aug. 1994.

[11] T. Ergodan, "Fiber grating spectra," *J. Lightwave Technol.*, vol. 15, pp. 1277–1294, Aug. 1997.

[12] C. Giles, "Lightwave applications of fiber Gragg gratings," *J. Lightwave Technol.*, vol. 15, pp. 1391–1404, Aug. 1997.

[13] M. W. McCall and A. Lakhtakia, "Polarization-dependent narrowband spectral filtering by chiral scupltered thin films," *J. Modern Opt.*, to be published.

[14] M. W. McCall and A. Lakhtakia, "Development and assessment of coupled wave theory of axial propagation in thin film helicoidal bianisotropic mediums. Part I: Reflectances and transmittances," *J. Modern Opt.*, to be published.

[15] P. St. J. Russell and J. L. Archambault, "Fiber gratings," in *Optical Fibers and Sensors—Components and Subsystems*, B. Culshhaw and J. Dakin, Eds. Boston, MA: Artech House, 1996, vol. 3.

Martin McCall received the B.Sc. degree from Imperial College, London, U.K., in 1983. He received the Ph.D. degree which was concerned with coupled wave theory in photorefractives, in 1987 while working at GEC.

After briefly working as a Postdoctoral Research Fellow at Bath University, U.K., he has been employed as a Lecturer at Imperial College since 1988. His research interests are mainly in optoelectronics and all aspects of grating physics.